Network-centered homeostasis through inhibition maintains hippocampal spatial map and cortical circuit function

Klara Kaleb, Victor Pedrosa, Claudia Clopath

Bioengineering Department, Imperial College London, London, United Kingdom

Abstract

Despite ongoing experiential change, neural activity maintains remarkable stability. Such stability is thought to be mediated by homeostatic plasticity and is deemed to be critical for normal neural function. However, what aspect of neural activity does homeostatic plasticity conserve, and how it still maintains the flexibility necessary for learning and memory, is not fully understood. Homeostatic plasticity is often studied in the context of neuron-centered control, where the deviations from the target activity for each individual neuron are suppressed. However, experimental studies suggest that there are additional, network-centered mechanisms. These may act through the inhibitory neurons, due to their dense network connectivity. Here we use a computational framework to study a potential mechanism for such homeostasis, using experimentally inspired, input-dependent inhibitory plasticity (IDIP). In a hippocampal CA1 spiking model, we show that IDIP in combination with place tuned input can explain the formation of active and silent place cells, as well as place cells remapping following optogenetic silencing of active place cells. Furthermore, we show that IDIP can also stabilise recurrent network dynamics, as well as preserve network firing rate heterogeneity and stimulus representation. Interestingly, in an associative memory task, IDIP facilitates persistent activity after memory encoding, in line with some experimental data. Hence, the establishment of global network balance with IDIP has diverse functional implications and may be able to explain experimental phenomena across different brain areas.

Introduction

Although neural activity varies, presumably due to different demands of various cognitive functions, it is usually constrained to a small operational range of only a few Hertz. This regime may facilitate energy saving (Perrinet 2010), as well as optimal information processing (Laughlin 1981, Stemmler & Koch 1999). Furthermore, deviations from this range are often associated with pathological states, such as epilepsy, schizophrenia, and Fragile X syndrome (Dickman & Wondolowski 2013). Given that neural activity undergoes constant experiential change, there exists a requirement for active processes to maintain stability. Many such processes have been identified, such as synaptic scaling (Turrigiano et al. 1998, Desai et al. 2002, Turrigiano & Nelson 2004, Goel & Lee 2007, Glazewski et al. 2017), intrinsic plasticity (Desai et al. 1999, Gainey et al. 2018, Lambo & Turrigiano 2013, Maffei & Turrigiano 2008), meta-plasticity (Bienenstock et al. 1982, Kirkwood et al. 1996, Zenke et al. 2013, Frank et al. 2006), diffusive neuromodulation (Sweeney et al. 2015, Steinert et al. 2008, 2011, Naumann & Sprekeler 2020), structural plasticity (Yin & Yuan 2015, Gallinaro & Rotter 2018) and inhibitory plasticity (Woodin et al. 2003, Maffei et al. 2004, 2006, Chen et al. 2011, Vogels et al. 2011, Keck et al. 2011, van Versendaal et al. 2012, D'amour & Froemke 2015, Udakis et al. 2019, Clopath et al. 2016, Hennequin et al. 2017, Das et al. 2011, Haas et al. 2006). These altogether make up the term homeostatic plasticity and, although vastly different, they all act as a negative feedback mechanism that adjust the neural parameters to compensate for deviations from some set-point. Homeostatic plasticity is often studied in the context of neuron-centered control, as neurons return to their preferred level of activity after experimental manipulations that decrease (Hengen et al. 2013) or increase activity (Pacheco et al. 2019). There is also experimental evidence of network-centered homeostasis (Hirase et al. 2001, Slomowitz et al. 2015, Trouche et al. 2016), where instead of the individual neurons, the mean activity of the whole network is homeostatically maintained . However, computational studies of such mechanisms are few (Sweeney et al. 2015, Naumann & Sprekeler 2020) and thus they remain less well understood.

To illustrate network-centered homeostasis, we turn to the hippocampus. Spatial environments are known to be represented by a cognitive map, consisting of a subset of hippocampal pyramidal cells. These are called place cells, as they fire action potentials when the animal is in a specific location within the environment, their place fields (O'Keefe & Dostrovsky 1971, O'Keefe 1976, O'keefe & Nadel 1978, Wilson & McNaughton 1993). Optogenetic silencing of the CA1 pyramidal neurons encoding a place map of a familiar environment leads to rapid activation of previously silent CA1 pyramidal neurons (Trouche et al. 2016). This abrupt increase is followed by a slower, seconds-long

2

activity change towards a stable level on par with that of the original place map (Trouche et al. 2016). Thus, an alternative place map transiently emerges while the original place cells are being silenced, and the spatial representation is homeostatically maintained. Furthermore, with repeated silencing, the alternative place map is consolidated over the original place map (Trouche et al. 2016). As neurons presumably have access only to their own activity, it is unclear how such a pertubation can be detected and compensated for at the network level.

One of the likely candidates to implement such network-centered homeostasis are the inhibitory neurons. CA1 inhibitory neurons are strongly connected to a large number of heterogeneously tuned CA1 pyramidal cells (Ali et al. 1998, Freund & Buzsaki 1996, Gulyás et al. 1999, Bezaire & Soltesz 2013, Csicsvari, Czurko, Hirase & Buzsaki 1998, English et al. 2017, Csicsvari, Hirase, Czurko & Buzsáki 1998), and exhibit broad spatial tuning (Grienberger et al. 2017). Thus, they can facilitate lateral inhibition between the pyramidal cells (Geisler et al. 2007) and as such, both sense and influence the activity of their local network. Hence, plasticity in the inhibitory circuitry could offer a highly efficient network activity homeostasis, which has previously been shown with neuron-centered plasticity (Vogels et al. 2011). However, there are indications that inhibitory plasticity can also act more globally. For instance, inhibitory postsynaptic potentials (iPSPs) have been shown to decrease when global, but not single neuron, spiking activity is suppressed (Hartman et al. 2006, Peng et al. 2010). Moreover, in the highly recurrent pyramidal cell networks of the neocortex, where inhibitory neurons are similarly interconnected with the rest of the network (Sohya et al. 2007, Niell & Stryker 2008, Kerlin et al. 2010, Ma et al. 2010, Zariwala et al. 2011, Znamenskiy et al. 2018, Wilson et al. 2017, Fino & Yuste 2011, Packer & Yuste 2011, Hofer et al. 2011, Bock et al. 2011, Pfeffer et al. 2013), inhibitory scaling was shown to be $Ca2+$/calmodulin-dependent protein kinase IV (CAMKIV) independent (Joseph & Turrigiano 2017), and thus may be decoupled from unique postsynaptic neuron activity. Furthermore, sensory deprivation studies across the primary cortices (Kuhlman et al. 2013, Barnes et al. 2015, Li et al. 2014, Gainey et al. 2018) have led to suggestions that inhibition could be broadly adjusted as a function of the activity of the circuit (Gainey & Feldman 2017). Inspired by all of these experimental findings, we hypothesize that the synaptic input to the inhibitory neurons could act as a proxy for the local network activity, and as such be used to adjust the level of inhibition appropriately.

In this work, we computationally study the properties and potential functionality of such novel inhibitory plasticity, which we term input-dependent inhibitory plasticity (IDIP). First, we show

that such plasticity provides a mechanistic explanation for the emergence of active and silent place cells in a hippocampal CA1 network model. Our model also reproduces the previously unexplained experimental data of fast and reversible remapping following acute optogenetic place map silencing (Trouche et al. 2016), as well as the consolidation of the alternative place map following repeated silencing (Trouche et al. 2016). Furthermore, we show that IDIP in a cortical recurrent network model provides a form of rapid firing rate homeostasis while maintaining important network features, such as firing rate heterogeneity and persistent activity. Thus, we show that IDIP allows for accurate maintenance of neural representation while preserving flexibility important for neural coding.

Results

Input-dependent inhibitory plasticity (IDIP) rule as a homeostatic mechanism

Experimental studies suggest an existence of network-centered homeostasis (Hirase et al. 2001, Slomowitz et al. 2015, Trouche et al. 2016), where the mean firing rate of the network, rather than that of the individual neurons, is homeostatically maintained. For example, rapid homeostasis of place representation in the hippocampal CA1 region is observed after optogenetic silencing of a familiar place map, through the emergence of an alternative place map (Trouche et al. 2016). The likely candidates underlying such a mechanism are the inhibitory neurons, due to their dense interconnectivity with the surrounding pyramidal cells, both in the hippocampus (Ali et al. 1998, Freund & Buzsaki 1996, Gulyás et al. 1999, Bezaire & Soltesz 2013, Csicsvari, Czurko, Hirase & Buzsaki 1998, English et al. 2017, Csicsvari, Hirase, Czurko & Buzsáki 1998) and in the neocortex (Sohya et al. 2007, Niell & Stryker 2008, Kerlin et al. 2010, Ma et al. 2010, Zariwala et al. 2011, Znamenskiy et al. 2018, Wilson et al. 2017, Fino & Yuste 2011, Packer & Yuste 2011, Hofer et al. 2011, Bock et al. 2011, Pfeffer et al. 2013). Furthermore, rapid disinhibition has been shown to be the first step in circuit reorganization after experimental deprivation across the sensory cortices (Kuhlman et al. 2013, Barnes et al. 2015, Li et al. 2014, Gainey et al. 2018), leading to suggestions that inhibition could be broadly adjusted based on the activity of the circuit (Gainey & Feldman 2017). Such global regulation of network activity could be achieved through the modulation of inhibition as a function of the synaptic input the inhibitory neurons receive. To this end, we hypothesize a plasticity mechanism in which strong inputs onto the inhibitory neurons lead to strengthening of the inhibitory output, whereas weak inputs onto the inhibitory neurons lead to weakening of the inhibitory output. For simplicity, we choose to implement this input-dependent inhibitory plasticity (IDIP) rule by scaling the inhibitory synaptic weights as a function of the difference between the actual and the target synaptic input that each inhibitory neuron receives (Fig 1.A). Note that such cell-autonomous plasticity could also be implemented through the plasticity of excitability of the inhibitory neurons, which is not explored in this work.

The IDIP rule allows for the emergence of active and silent place cells in a hippocampal network

To assess whether IDIP can lead to the emergence of active and silent place cells, we build a hippocampal network model of leaky integrate-and-fire neurons. The network model consists of the CA3 and CA1 region (Fig 1.B). Each pyramidal cell in the CA3 region receives unique place tuned external current (Fig S1.A-B), representing the location of a simulated mouse on a 1D annular track with equally spaced place fields. The CA3 neurons project to the CA1 excitatory neurons, which are divided into equally sized groups, with neurons in each group tuned to the same place field. As the CA1 excitatory neurons are poorly recurrently connected (Deuchars & Thomson 1996, Thomson & Radpour 1991), in our simulations we assume that there are no recurrent connections between them. The CA1 excitatory neurons project to the CA1 inhibitory neurons and the CA1 inhibitory neurons project back to the CA1 excitatory neurons. The CA1 inhibitory neurons have no spatial tuning (Fig S2.A), in agreement with experiments (Dupret et al. 2013, Grienberger et al. 2017). The excitatory synapses between the CA3 and CA1 excitatory neurons and the inhibitory synapses to the CA1 excitatory neurons are made plastic with Hebbian plasticity and the IDIP rule respectively.

We first wanted to test whether IDIP could allow for the emergence of both active and silent place cells in the CA1 region. The experiments suggest that the cells which later become active or silent are differentiable even before the first exploration of the environment (Epsztein et al. 2011). We incorporate this in our model by introducing variability in the amplitude of the place tuning of the CA1 excitatory neurons belonging to the same group (Fig 1.C-D, Fig S3.A-B). As the initial inhibitory synaptic weights are set to low values, all the CA1 excitatory neurons are active, covering the whole environment (Fig 1.E). We then let our simulated mouse complete 100 laps on the track, which we term the exploration phase. During this phase, the CA1 excitatory neurons that are highly place tuned are potentiated more. Through activity, their tuning also increases in a positive feedback loop characteristic to Hebbian learning (Fig 1.F-G, Fig S3.C-D). This increases the synaptic input to the CA1 inhibitory neurons, and hence increases the inhibitory synaptic weights through IDIP (Fig S2.B). As the CA1 excitatory neurons with lower place tuning are less active, they are unable to escape the increasing lateral inhibition. Thus stable active and silent place cells form within each CA1 group (Fig 1.H, Fig S3.E-F). The absence of the target firing rate for individual excitatory neurons is essential for this. Hence, we show that the IDIP rule together with Hebbian plasticity and place tuned inputs can explain the formation of active and silent place cells in a hippocampal network model.

6
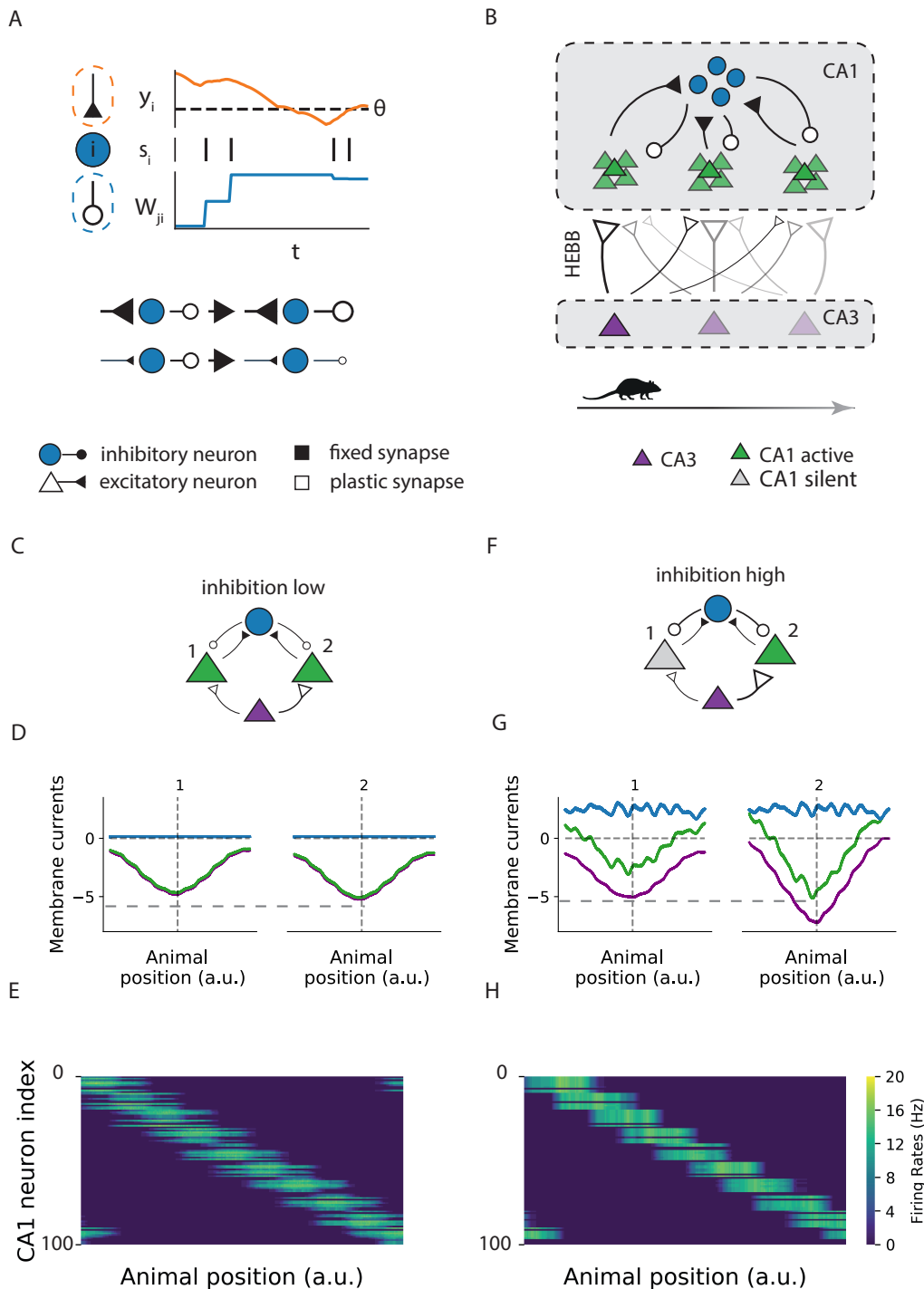
Figure 1. The IDIP rule enables emergence of active and silent place cells in a hippocampal network. A. Diagram of the inhibitory plasticity rule. An inhibitory neuron (blue) adjusts its projecting inhibitory synaptic weights based on the synaptic current it is receiving. Strong inputs onto inhibitory neurons lead to strengthening of inhibitory output weights, whereas weak inputs onto inhibitory neurons lead to weakening of inhibitory output weights. **B.** Hippocampal network diagram. The CA3 region consists of 10 excitatory neurons (purple triangles). Each receives unique place-dependent external current, representing the location of a

simulated mouse on a 1D annular track with equally spaced place fields. CA3 neurons project to 100 CA1 excitatory neurons (green triangles). These are split in 10 equally sized groups, with neurons in each group tuned to the same place field. CA1 excitatory neurons project to CA1 inhibitory neurons (blue circles) , which in turn project back to the CA1 excitatory neurons. The excitatory synapses from the CA3 to the CA1 are plastic under Hebbian plasticity and the inhibitory synapses in the CA1 are plastic under IDIP. **C-E** State of the network during the first lap, before any learning. **C.** A diagram of a sample microcircuit found in the network **B**, consisting of 2 CA1 excitatory neurons (1 and 2) with the same spatial tuning, but with neuron 2 having slightly larger CA3 to CA1 synaptic strengths. **D.** The excitatory (purple), inhibitory (blue) and net (green) currents received by neurons 1 and 2 during the first lap on the track. The higher peak net current received by neuron 2 reflects its higher place field tuning compared to neuron 1. **E.** The firing rates of all the excitatory neurons in the CA1 network (y-axis) during the first lap on the simulated track (x-axis). All the place cells are active but with varying amplitudes, reflecting differences in their place tuning strengths. **F-H** Same as in B-D, but after inhibitory and excitatory learning (100 laps). **F.** The same microcircuit diagram as in **C** but after learning. The CA3 to CA1 excitatory synaptic plasticity leads to increased activity of both neurons. Due to the differences in their tuning, the excitatory synapses to neuron 2 are potentiatied more. At the same time, increased activity in the CA1 excitatory neurons increases input to the inhibitory neurons, and thus the inhibitory synaptic weights are increased as well. This increased inhibition eventually completely overcomes excitation in the less active neuron 1 and hence it becomes a silent place cell (grey). **G.** Excitatory (orange), inhibitory (blue) and net (green) currents received by neurons 1 and 2 during the last lap on the track. The difference in the peak net currents from the first lap **D** is amplified with learning. **H.** The firing rates of all the excitatory neurons in the CA1 network (y-axis) during the last lap on the simulated track (x-axis). The place cells have a well defined place field and a subset of cells within each place tuned group have become silent.

The IDIP rule enables rapid homeostatic remapping during active place cells silencing

To assess whether the proposed IDIP rule can facilitate rapid place cell remapping, we perform a silencing protocol as in Trouche et al. (2016) (Fig 2.A). After the exploration phase, we tag all the established active place cells and silence them. In the networks with (Fig 2.B) and without (Fig. 2.F) IDIP, such silencing leads to a decrease in the excitatory drive to the CA1 inhibitory neurons and subsequently a rapid decrease in the inhibition to the previously silent place cells, which then form an alternative place map. However, the degree of the alternative place map activation will depend on inhibitory plasticity. In the networks with IDIP during the silencing (Fig 2.B), the dynamics of the alternative place map activation are similar to that observed experimentally (Fig 2.C) (Trouche et al. 2016). The firing rates of the alternative place cells are first increased almost immediately after silencing onset (fast phase) and are further increased within the next 1-2 seconds (slow phase) (Fig 2.D). Our model allows us to decompose the two phases. The fast phase is due to the rapid decrease in CA1 inhibitory neuron firing rate (Fig S4.A), as the originally active place cells, which were driving their activity, are no longer active. Thus the alternative place map emerges, but at a lower firing rate than the original place map, due to the place cells forming the alternative place map being less sharply place-tuned than the place cells that formed the original place map. In the networks without IDIP during the silencing (Fig 2.F), the activity of the alternative place map does not progress beyond this phase (Fig 2.G-H). However, in the networks with IDIP during the silencing, a second, slower phase of alternative map activation occurs as the level of inhibition gets adjusted to the lower activity and thus lower synaptic input from the alternative place cells (Fig S4.B) . Therefore the final activity of the alternative place map matches that of the original place map (Fig 4.E). Hence, the IDIP rule acts as a homeostatic mechanism to maintain network activity during acute silencing.

When we turn silencing off, the original place map re-emerges (Fig 2.C), in agreement with experiments (Trouche et al. 2016). However, repeating the silencing protocol (Fig 2.I) consolidates the alternative place map (Fig 2.J), also in agreement with experiments (Trouche et al. 2016). In our model this happens through the gradual activity-dependent Hebbian plasticity in the CA3 to CA1 excitatory synapses (Fig S5.A). Therefore, our model suggests that synaptic plasticity of feedforward inputs onto the CA1 pyramidal cells is a good candidate for the mechanism underlying place map consolidation.

9
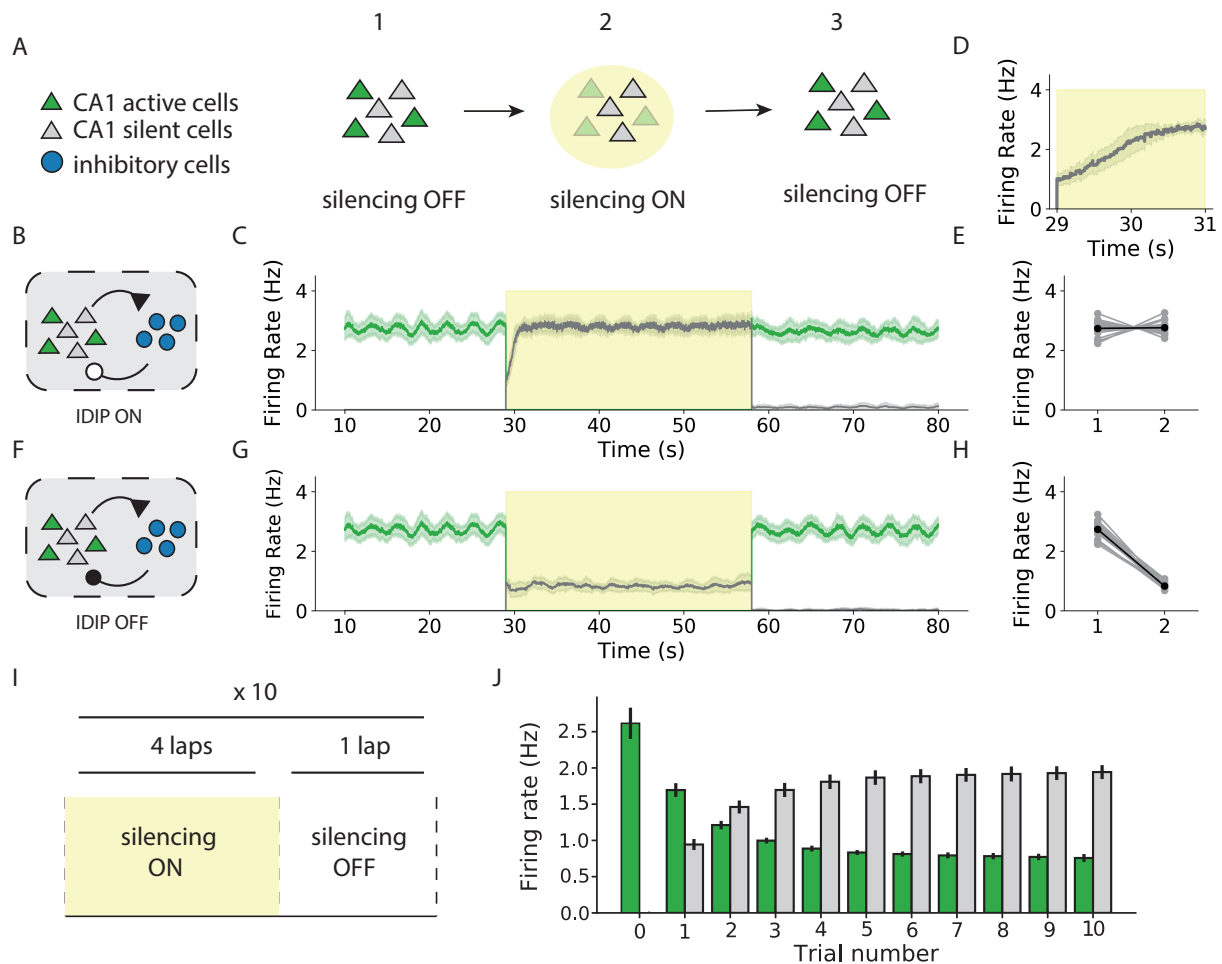
Figure 2. Place cells silencing leads to a rapid emergence of an alternative place map.

A. Silencing protocol similar to Trouche et al. (2016). All the active cells (green) are tagged (1), silenced for one lap (2) and released in the subsequent lap (3). **B-E** Silencing in the network following IDIP. **B.** Network diagram after the exploration phase (100 laps). **C.** Mean firing rate of the network just before (1), during (2), and after silencing (3). During silencing (2) there is rapid activation of an alternative place map, consisting of the previously silent cells (grey). After silencing (3), the original map reactivates (green). **D.** Alternative place map activation just after silencing. **E.** The mean firing rate of the place map before (1) and during (2) silencing. Gray circles indicate individual trials. Black circles indicate average over all 20 trials. **F-H** Same as in **B-E** but with inhibitory plasticity turned off during silencing (2). **F.** Network diagram after inhbitory and excitatory learning (lap 100) with IDIP turned off during silencing (2). **G.** Without IDIP during the silencing (2) there is low alternative place cell activation. **H.** Without IDIP during the silencing (2) the mean firing rate of the place map decreases. Gray circles indicate individual trials. Black circles indicate average over all 20 trials. **I** Consolidation protocol similar to Trouche et al. (2016). The established place map is silenced for 4 consecutive laps, and then released for a single testing lap. This is repeated for 10 trials. **J.** Mean firing rate of the active (green) and silent (grey) place map during the testing laps at each trial. Trial 0 corresponds to the activity of the network just after the exploration phase.

The IDIP rule establishes global E/I balance in recurrent networks

The inhibitory neurons also feature dense connectivity in the neocortical circuits (Sohya et al. 2007, Niell & Stryker 2008, Kerlin et al. 2010, Ma et al. 2010, Zariwala et al. 2011, Znamenskiy et al. 2018, Wilson et al. 2017, Fino & Yuste 2011, Packer & Yuste 2011, Hofer et al. 2011, Bock et al. 2011, Pfeffer et al. 2013) and there is some evidence for a network-centered control of cortical activity through inhibition (Joseph & Turrigiano 2017, Gainey & Feldman 2017, Gainey et al. 2018). To assess whether the proposed IDIP learning rule can homeostatically regulate such circuits, we simulate a cortical network of leaky integrate-and-fire neurons with sparse recurrent connectivity (Fig 3.A). Each neuron in the network receives large external excitatory input and the initial inhibitory synaptic weights are set to low values. Thus, without any plasticity, the network exhibits pathologically high activity (Fig 3.B). Due to the high activity of the network, the inhibitory neurons initially receive very large excitatory synaptic input, and thus the IDIP rule increases the inhibitory synaptic weights (Fig 3.B - IDIP turned on at 15s, Fig S6.A). The network, therefore, progresses from a high synchronous to a low asynchronous firing following the IDIP rule (Fig 3.E). The excitatory firing rates reach a more physiological regime (Fig 3.B, Fig S6.B), with a reasonable firing rate distribution and irregular firing rate dynamics (Fig 3.C). Inhibitory neurons in the network also exhibit a diversity of firing rates and irregular firing rate dynamics (Fig S7.A-E). Hence, IDIP can homeostatically regulate network-wide activity.

The IDIP rule proposed does not impose a unique target firing rate for each neuron in the network. Instead, it controls the mean firing rate across the whole network. The final variability in the net current received by each individual excitatory neuron after inhibitory learning (Fig 3.F) results in a diversity of neuronal firing rates (Fig 3.C). This is in contrast with the network following a neuron-centered rule, such as inhibitory spike-timing dependent plasticity (iSTDP) (Vogels et al. 2011), which effectively sets a target firing rate for the excitatory neurons (Fig S8.A-E). To assess the range of the firing rates the IDIP rule can support in a recurrent network, we simulate the network for various values of the inhibitory target input. Higher values of the inhibitory target input lead to higher network activity (Fig 3.D, y-axis). Hence, the activity of the network following the IDIP rule depends on the target input of the inhibitory neurons. Altogether, this means that IDIP establishes a global, rather than detailed, network excitatory (E)/ inhibitory (I) balance while allowing for network diversity.

11
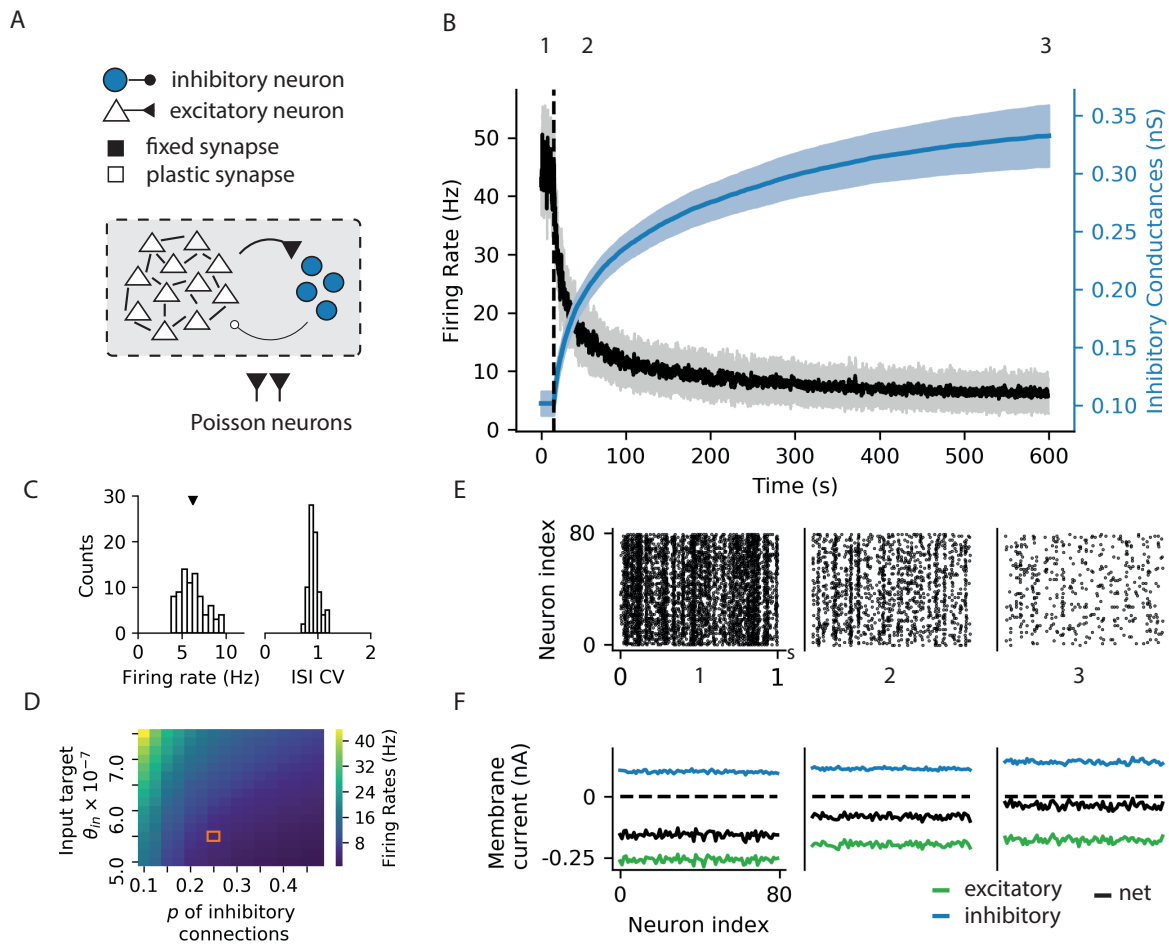
Figure 3. IDIP establishes global E/I balance in recurrent networks. **A.** A recurrent network of 80 excitatory (white triangles) and 20 inhibitory (blue circles) leaky integrate-and-fire neurons receiving external input from a pool of 100 Poisson excitatory neurons. Only the inhibitory synaptic weights are made plastic with IDIP. **B.** The evolution of the mean excitatory firing rate (black) and the mean inhibitory weight (blue) of the network. Shaded regions correspond to the standard deviation of individual units. IDIP is turned on at 15s (dashed vertical line). Activity of the network decreases as inhibitory weights increase. **C.** The excitatory firing rate stabilises to a mean value of 6.2 Hz (left, black triangle). The network displays an asynchronous firing pattern (right). **D.** The range of mean network firing rates IDIP can support, with varying input target value (y-axis) and inhibitory connectivity (x-axis). The orange square marks the parameters used in our simulations. **E.** Spike raster plots at the time points marked in **B**. The network progresses from high synchronous to low asynchronous firing following the IDIP rule. **F.** Mean membrane currents as a function of excitatory neuron index at the time points marked in **B**.

12

The IDIP rule enables maintenance of neural representations

We wanted to assess whether neural representation could be maintained in the networks following the IDIP rule. To assess whether individual neurons can remain highly active, we increase the external drive to a subset of neurons in the network (Fig 4.A). The selected subset sustains a higher firing rate relative to the rest of the network following inhibitory learning with IDIP (Fig 4.B, S9.A). This effect is mediated by the highly active neural subset monopolizing the input to the inhibitory neurons, leading to greater inhibition to the rest of the network. Thus the rest of the network compensates for this increased activity, as seen in a slight decrease in the mean network firing rate (Fig 4.C). As expected, the deviations from the target excitatory neuron firing rate are suppressed in the network following iSTDP (Vogels et al. 2011) (Fig S9.B). Hence, IDIP can control the recurrent network activity while preserving activity heterogeneity.

To assess whether the relative firing rates between neurons can be conserved across the whole neural population, we rank the firing rates of the neurons at the beginning of our simulations, before any inhibitory plasticity (Fig 4.D). We then measure whether this rank is maintained over time following inhibitory plasticity (Fig 4.D). In networks following IDIP, the firing rate rank correlation is largely conserved after inhibitory learning (Fig 4.E, Fig S9.C). We compare this with the network following iSTDP (Vogels et al. 2011), where the firing rate rank correlation is mostly lost, as all neurons fire at similar firing rates at the end of the simulations (Fig 4.E, Fig S9.D). Hence, IDIP can preserve heterogeneity in firing rates, both at a single neuron level and across the whole network.
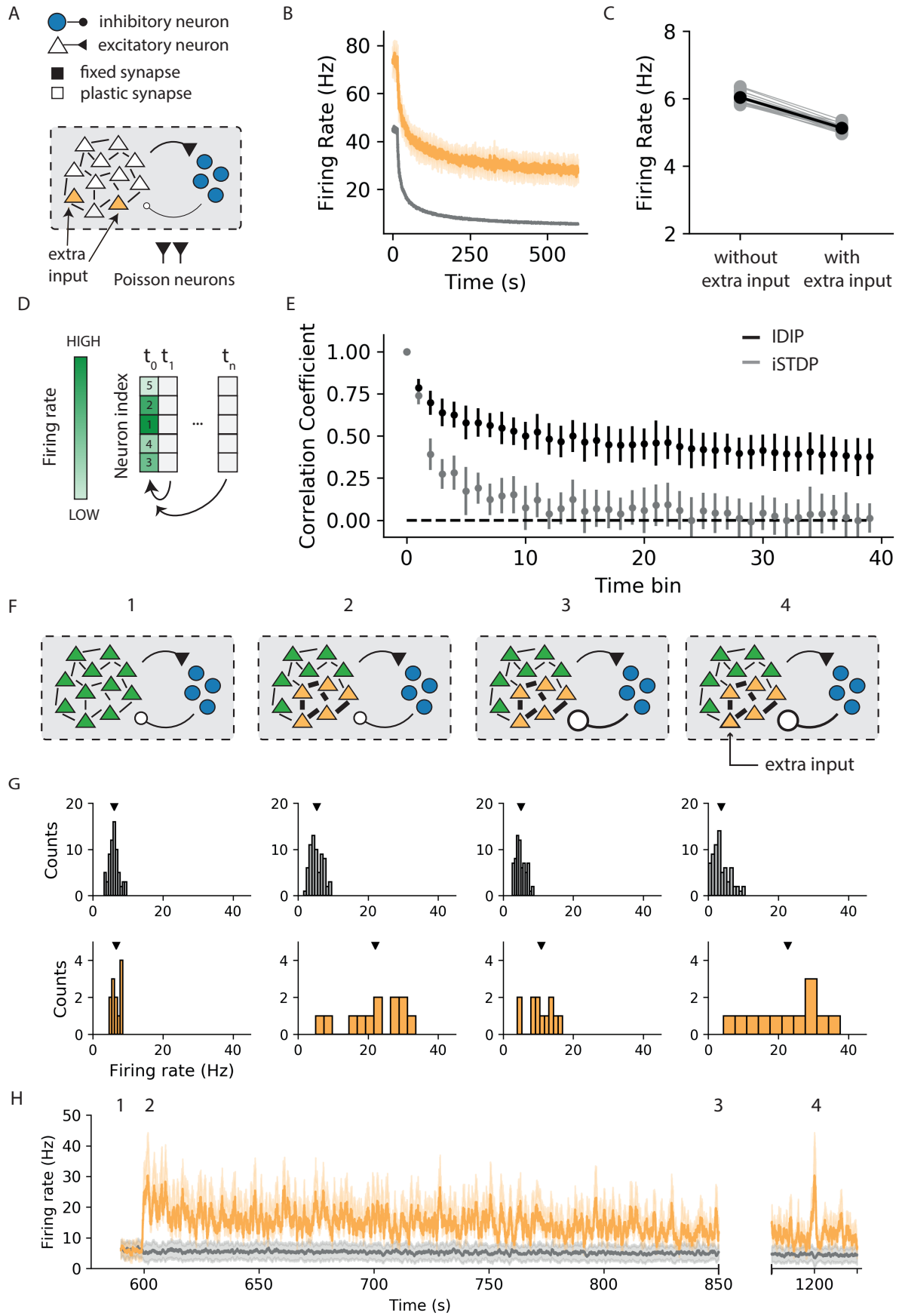
The IDIP rule enables memory trace persistence and recall

We also assess the performance of the network following IDIP in a simple associative memory task. Once the network activity stabilises, we encode a memory by increasing the recurrent excitatory connections within a pattern in the network (Fig 4.F), as previously done in networks following iSTDP (Vogels et al. (2011), reproduced in Fig S10.C-D). After encoding, the neurons recruited to the memory pattern exhibit sustained activity which is higher than the rest of the network, even after IDIP has converged (Fig 4.G-H, Fig S10.A). This is in contrast to the networks following iSTDP (Vogels et al. 2011), in which the activity of the memory ensemble becomes indistinguishable from the rest of the network at convergence (Fig S10.C-D). Such persistent activity of the memory cells has been reported in some experiments (Yassin et al. (2010), Ghandour et al. (2019), but see Barron

et al. (2017)).

We then test whether we can recall the pattern, given that IDIP made inhibition stronger in the network. By increasing the external current to some units in the pattern, the memory can be re-called (Fig 4.G-H, Fig S10.B). Performing the same protocol in a network following iSTDP (Vogels et al. 2011) shows that a lower number of memory cells are re-activated with recall (Fig S10.C). Thus recall in the network following IDIP has higher fidelity. This is in line with experiments (Pignatelli et al. 2019), where increased activity of the memory cells facilitates greater pattern completion. Hence, the IDIP rule allows for sustained activity of memory cells after encoding, as well as faithful memory recall from a partial cue.

In summary, we show that our proposed inhibitory plasticity rule, IDIP, can homeostatically regulate activity in models of hippocampal and cortical networks. Importantly, using IDIP we are able to reproduce previously unexplained experimental findings in the hippocampus (Trouche et al. 2016) and propose its potential functional implications in the recurrent cortical networks.

Figure 4. IDIP rule enables maintenance of neural representations and memory trace persistence. **A-C.** Perfomance of the IDIP rule in networks with heterogeneous activity. **A.** The same network as in Fig 3.A, but with a subset of neurons receiving increased external input. **B.** The average firing rates of the networks with increased input as in **A**. Bold lines denote the average and the shaded area indicated standard deviation over 20 trials. The increased activity relative to the rest of the network is sustained after inhibitory learning with IDIP. **C.** The average firing rate of the networks without (left) and with (right) input heterogeneity. Gray circles indicate individual trials and the black circles indicate average over all 20 trials. **D-E.** Performance of IDIP and iSTDP (Vogels et al. 2011) in a network representation task. **D.** Network representation task diagram. We calculate the preservation of the correlation with the initial rank of firing rates during the entire course of the simulation. **E.** The Spearman rank correlation coefficient for the network following IDIP (black) and iSTDP (grey). Error bars correspond to standard deviation over 20 trials. The horizontal dashed line indicates no correlation. **F-H.** Perfomance of the IDIP rule in an associative memory task. **F.** Associative memory task protocol. Following network stabilization (1), we increase recurrent excitatory connections between a subset of neurons (2). This leads to increase in inhibition (3). The encoded assembly is recalled by increasing external input to a subset of neurons within the pattern (4). **G.** Histograms of average firing rates of the assembly (orange) and the rest of the network (grey) at the marked task time points **F**. The black triangles indicate the mean firing rates. **H.** The evolution of the firing rates of the assembly (orange) and the rest of the network (grey) during the memory task. The shaded area indicates standard deviation over all units in each network subset.

Discussion

Although the study of neural homeostasis is frequently neuron-centered, there is some evidence that network-centered mechanisms are also at play (Hirase et al. 2001, Slomowitz et al. 2015, Trouche et al. 2016). One of the candidates proposed for the implementation of such homeostasis are the inhibitory neurons, due to their dense connectivity, both in the hippocampus (Ali et al. 1998, Freund & Buzsaki 1996, Gulyás et al. 1999, Bezaire & Soltesz 2013, Csicsvari, Czurko, Hirase & Buzsaki 1998, English et al. 2017, Csicsvari, Hirase, Czurko & Buzsáki 1998), as well as in the neocortex (Sohya et al. 2007, Niell & Stryker 2008, Kerlin et al. 2010, Ma et al. 2010, Zariwala et al. 2011, Znamenskiy et al. 2018, Wilson et al. 2017, Fino & Yuste 2011, Packer & Yuste 2011, Hofer et al. 2011, Bock et al. 2011, Pfeffer et al. 2013). In this work, we take inspiration from the experimental data and hypothesize that network homeostasis could be achieved through input-dependent inhibitory plasticity (IDIP), in which the inhibition is adjusted as a function of the synaptic input the inhibitory neurons receive. We show that in a hippocampal CA1 network model, IDIP can provide a mechanistic circuit understanding and reproduce experimental data in which place cells are optogenetically silenced, unmasking a previously silent place map (Trouche et al. 2016). Furthermore, we show that such a learning rule can also homeostatically regulate the activity of a recurrent neural network, while preserving flexibility important for neural coding. Altogether, our results suggest that network activity homeostasis following external manipulation or endogenous changes could share a common underlying mechanism.

In contrast to the commonly used neuron-centered inhibitory plasticity (Vogels et al. 2011), the IDIP rule features an absence of a target firing rate for each excitatory neuron. Instead, with the IDIP rule, the level of inhibition is modulated to maintain the mean firing rate of the whole network. The importance of this is seen in our data-driven model of the CA1 network, where IDIP allows for emergence of both active and silent place cells. In our model, these emerge as the neurons with higher activity dominate the input to the inhibitory neurons, and thus the recruitment of lateral inhibition. Conversely, the less active cells become silent. Thus, there is an amplification of slight differences in activity through scaling of the tonic inhibition, indiscriminately to all cells. Such competition for the recruitment of inhibition has previously been suggested to shape hippocampal assemblies (Buzsáki 2010). Furthermore, silencing of an established place map induces rapid compensatory adjustment of inhibition, and thus an emergence of an alternative place map (Fig 2.C), as reported experimentally (Trouche et al. 2016). We show that non-plastic inhibition is not consistent with the experimental data (Fig 2.G). Finally, we show that repeated silencing leads to

alternative place map consolidation (Fig 2.J), as reported experimentally (Trouche et al. 2016). In our model, this occurs through gradual changes in the CA3 to CA1 excitatory synaptic weights (Fig S5), facilitated by disinhibition during each silencing lap (Fig S4.A). Thus, through time, the original place map gets destabilised, which has previously been suggested as a necessary condition for remapping (Schoenenberger et al. 2016). Hence, network-centered homeostasis through IDIP provides a possible explanation for the previously unexplained experimental phenomena in the hippocampus.

We also assess whether IDIP can homeostatically regulate dynamics in the recurrent networks typical of the neocortex. Due to the absence of a firing rate set-point in the networks following IDIP, there is diversity in the neuronal firing rates within the recurrent network after inhibitory learning (Fig 3.C). The resulting firing rate distribution is consistent with the broad and heavy-tailed distribution of firing rates observed experimentally (Wohrer et al. 2013), with some neurons more active than others (Mizuseki & Buzsáki 2013). Such range of activity is thought to be optimal for the information storage in the brain (Laughlin 1981) and enables linear network responses over a broad range of inputs (Sweeney et al. 2015). In our networks, highly active neurons dominate synaptic input to the inhibitory neurons, recruit inhibition more and thus inhibit other neurons more. Hence with the IDIP rule, highly active neurons can remain so as long as the rest of the network can compensate for it, providing a more flexible control. We illustrate this when we increase the external inputs to some neurons and they remain consistently more active than the rest of the network (Fig 4.B). Furthermore, we show the IDIP rule can also extend this stability of the firing rate rank across the whole neural population (Fig 4.E). This is not the case with inhibitory spike-timing dependent plasticity (iSTDP) (Vogels et al. 2011), as the ranks get shuffled following inhibitory learning, due to the unique firing rate set-point constraint (Fig 4.E). Hence, the IDIP model can maintain the population firing rate around a target value while preserving neural representation. Importantly, the neural activity diversity is not imposed but emerges due to random network structure. Although such population heterogeneity can be imposed, this has been previously shown to lead to limited network responsiveness (Sweeney et al. 2015). Hence, IDIP provides a global control of recurrent network dynamics, without a firing rate set-point for each neuron, which allows for flexibility and thus conservation of network representation.

Additionally, in an associative memory task, we show that the networks following the IDIP rule can sustain memory encoding, without disturbing the rest of the network (Fig 4.F-G). This has

previously also been shown with iSTDP (Vogels et al. 2011). However, the key difference is that networks following the IDIP rule exhibit persistent activity of assemblies after encoding (Fig 4.G-H), unlike iSTDP (Fig S10.C-D), as well as higher fidelity of recall (Fig 4.G-H). Persistent activity of the memory cells has been reported in some experiments (Yassin et al. (2010), Ghandour et al. (2019), but see Barron et al. (2017)) and is thought to be involved in memory bindings via Hebbian plasticity, as the increased activity further strengthens the memory trace (Han et al. 2007) and facilitates greater recall (Tonegawa 2019). Thus, the global network control provided by IDIP may have important functional implications in memory processing and recall.

As highlighted throughout this work, dense connectivity of the inhibitory neurons to their local networks makes them an ideal candidate for network-centered homeostasis. However, more sparsely connected networks would lead the inhibitory neurons to sense a subset of the network and potentially affect a different subset. Thus the final network firing rate would be less constrained (Fig 3.D, Fig S11). This suggests that the network activity is differentially modulated by the IDIP rule depending on the network architecture. In the limit of very sparse networks, IDIP may not even act as a homeostatic mechanism and winner-take-all dynamics may dominate (Fig S12). This may be relevant in the prevention of redundancy or in contrast enhancement (Hartline & Ratliff 1957). Furthermore, inhibitory connectivity is known to vary within (Meyer et al. 2011) and between (Tamamaki & Tomioka 2010) brain areas. Thus, IDIP rule would have different functional consequences in different brain regions.

The basis of our proposed IDIP rule is that the inhibitory neurons, presumably fast-spiking parvalbumin (PV+) cells, can sense and affect the network activity through their input and output synaptic connections respectively. Input integration over the timescale used in our model could be mediated through N-methyl-D-aspartate receptors (NMDARs), which are known to enhance the neuronal computational repertoire (Gasparini & Magee 2006, Losonczy & Magee 2006, Poirazi & Mel 2001, Stuart & Spruston 2015, Poirazi & Papoutsi 2020). In the hippocampus, NMDAR knockouts in the PV+ cells disrupt spatial representation (Korotkova et al. 2010) and NMDAR were also shown to be preferentially localized at feedback synaptic inputs to the PV+ cells (Le Roux et al. 2013). NMDAR have also recently been shown to facilitate supralinear dendritic integration in the PV+ cells (Cornford et al. 2019), a model of which also shows winner-take-all dynamics between distinct assemblies (Cornford et al. 2019). Furthermore, in the prefrontal cortex, application of NMDAR antagonists causes disinhibition (Homayoun & Moghaddam 2007, Jackson et al. 2004, Zhang

et al. 2008), initially caused by decrease in the inhibitory neuron activity (Homayoun & Moghaddam 2007), possibly via changes in their excitability, with prolonged exposures modulating the synthesis of gamma-Aminobutyric acid (GABA) (Zhang et al. 2008). Inhibitory output has also been shown to be modulated by activity, through modulation of rate limiting enzymes of GABA synthesis (Lau & Murthy 2012) or GABA transporters (De Gois et al. 2005). Such plasticity mechanisms have also recently been reported in the chandelier cells (Pan-Vazquez et al. 2020) and striatial inhibitory neurons (Paraskevopoulou et al. 2019) during development. Altogether, these studies indicate that our model of tonic inhibition modulated as a function of synaptic input to the inhibitory neurons is a biologically plausible mechanism.

Finally, other distinct solutions have been proposed for network-centered homeostasis, such as diffusive neuromodulation via nitric oxide (Sweeney et al. 2015) and GABA spillover (Naumann & Sprekeler 2020). It is very likely that they all coexist, alongside other, neuron-centered homeostatic mechanisms. Each homeostatic mechanism may control distinct aspects of neural function, as shown in a recent computational study (Wu et al. 2019). Hence, it would be of future interest to study the IDIP rule in conjunction with other homeostatic plasticity rules, such as synaptic scaling (Turrigiano et al. 1998, Desai et al. 2002, Turrigiano & Nelson 2004, Goel & Lee 2007, Glazewski et al. 2017), intrinsic plasticity (Desai et al. 1999, Gainey et al. 2018, Lambo & Turrigiano 2013, Maffei & Turrigiano 2008), metaplasticity (Bienenstock et al. 1982, Kirkwood et al. 1996, Zenke et al. 2013, Frank et al. 2006), diffusive neuromodulation (Sweeney et al. 2015, Steinert et al. 2008, 2011, Naumann & Sprekeler 2020), structural plasticity (Yin & Yuan 2015, Gallinaro & Rotter 2018) and inhibitory plasticity (Woodin et al. 2003, Maffei et al. 2004, 2006, Keck et al. 2011, Chen et al. 2011, Vogels et al. 2011, van Versendaal et al. 2012, D'amour & Froemke 2015, Udakis et al. 2019, Clopath et al. 2016, Hennequin et al. 2017, Das et al. 2011, Haas et al. 2006), as their interaction may increase the compensatory repertoire of the networks and endow them with non-trivial emergent properties.

Methods

Neuron Model

We use the single compartment leaky integrate-and-fire neuron model in our simulations. The model is defined by a resting membrane potential V_{REST} and membrane time constant τ_m. If the membrane potential surpasses the set threshold potential θ_m, it fires a spike and its membrane potential is reset back to V_{REST}. It then enters the refractory period t_{ref}, during which it cannot be stimulated.

The sub-threshold membrane voltage V_i of neuron i follows:

$$\tau_m \frac{dV_i}{dt} = (V_{REST} - V_i) + R(g^E(V^E - V_i) + g^I(V^I - V_i) + I_{ex}) \tag{1}$$

where R is the membrane resistance, $g_{E/I}$ are the excitatory and inhibitory synaptic conductances, $V^{E/I}$ are excitatory and inhibitory reversal potentials and I_{ex} is any other externally supplied current. If neuron i receives input from neuron j, the corresponding synaptic conductance g_{ij} is follows:

$$\tau_{E/I} \frac{dg_{ij}}{dt} = -g_{ij} + \bar{g} W_{ij} \delta(t - t_{spike}) \tag{2}$$

where $\tau_{E/I}$ is the synaptic time constant, W_{ij} is the synaptic weight, $\bar{g}$ is a basic unit of synaptic conductance and t_{spike} is the time of the presynaptic spike.

Input-dependent inhibitory plasticity (IDIP)

The inhibitory plasticity depends on the input current y_i received by each inhibitory neuron i over time.

$$\tau_{IDIP} \frac{dy_i}{dt} = -y_i + \sum_j g^E_{ij}(t) S_j(t) \tag{3}$$

where τ_{IDIP} is the input current time constant, g^E_{ij} is the excitatory synaptic conductance of the synapse from an excitatory neuron j to an inhibitory neuron i and $S_j(t)$ is the spike train of the excitatory neuron j. Hence the second term is the sum of all of the excitatory input currents to the inhibitory neuron i at time t. When the inhibitory neuron i spikes, all the inhibitory synapses

projecting from the presynaptic inhibitory neuron i to the postsynaptic excitatory neuron j are adjusted with respect to y_i as:

$$\Delta w_{ji} = \eta_{IDIP}(y_i(t) - \theta_{in}) \tag{4}$$

where η_{IDIP} is the inhibitory learning rate and θ_{in} is the constant target input for each inhibitory neuron. In our simulations, θ_{in} is the same for all inhibitory neurons.

Hippocampal Network Model

We simulate a CA1 network consisting of N_E excitatory neurons and N_I inhibitory neurons. There is full and bidirectional connectivity between the excitatory and inhibitory neurons. The initial synaptic weights from the inhibitory to the excitatory neurons (W_{IE}) are 200 times weaker than the synaptic weights from the excitatory to the inhibitory neurons (W_{EI}) . The initial values of the inhibitory synaptic weights are set to ten times weaker than the excitatory weights. The CA1 excitatory neurons are divided in N_g equally sized groups.

Each excitatory neuron in the CA1 network is connected to N_{CA3} CA3 neurons. The excitatory synaptic weights from the CA3 neurons to the CA1 excitatory neurons are made plastic with classical Hebbian plasticity and the inhibitory synaptic weights from the CA1 inhibitory neurons are made plastic with IDIP.

Position-modulated inputs

We model a mouse traversing a 1D annular track with N_{pc} equally spaced place fields. We assume the mouse moves with a constant speed and takes 3 seconds to move from a centre of one place field to a centre of the subsequent place field.

Each CA3 neuron receives input from one unique place field in the form of an external current I_{ex}. The tuning curve T with place field centered at p_0 is defined as:

$$T(p) = exp\left(-\frac{(p - p_0)^2}{2\sigma_{pc}^2}\right) \tag{5}$$

where p is the animal's position and σ_{pre} is the tuning width.

The place field current I_{ex} supplied to a CA3 neuron is then:

$$I_{ex}(p) = A_c T(p) \tag{6}$$

22

where A_c is the current amplitude.

Each CA1 group is tuned to a single unique CA3 neuron, with the same tuning curve T as in Eq. 5. Within group, the tuning amplitude for each neuron is varied. To this end, we sample a vector of $\frac{N^E}{N_g}$ random number from a normal distribution with $\mu = 0$ and $\sigma = 0.05$. We then shuffle this vector for each group and add a single value to the synaptic tuning curve of each neuron in the group.

The excitatory and inhibitory CA1 neurons also receive uniform external currents, I_{ex}^E and I_{ex}^I respectively.

Excitatory plasticity

The excitatory synaptic weights between CA3 and CA1 excitatory neurons follow classical Hebbian plasticity implemented using a symmetrical spike-timing dependent learning rule. A synaptic trace x_i assigned to each neuron i and follows:

$$\tau_{hebb} \frac{dx_i}{dt} = -x_i + \delta(t - t_{spike}) \tag{7}$$

where τ_{hebb} is the time constant of the learning window and t_{spike} is the spike time. We also include a homeostatic term which takes into account the sum of all synaptic weights onto the postsynaptic neuron. The synaptic weight w_{ji} from the presynaptic neuron j to the postsynaptic neuron i is updated following:

$$\frac{dw_{ji}}{dt} = (W_{max} - w_{ji})\eta_{hebb} x_i x_j - \eta_{homeo} \left(\sum_i w_{ji} - \theta_{homeo} \right) \tag{8}$$

where W_{max} is the maximum excitatory synaptic weight, η_{hebb} is the learning rate of the Hebbian term, η_{homeo} is the learning rate of the homeostatic term and θ_{homeo} is the homeostatic target.

Recurrent Network Model

We simulate a recurrent network consisting of N_E excitatory and N_I inhibitory neurons. The excitatory neurons are randomly connected with a probability $p_{EE} = 0.1$, in line with experiments (Harris & Shepherd 2015). The inhibitory neurons are randomly connected to the excitatory neurons with a probability $p_{IE} = p_{EI} = 0.2$. Due to the small size of the network, the *in* degree for

each excitatory and inhibitory neuron is kept the same. Thus each excitatory neuron has $N_E \times p_{EE}$ excitatory inputs and $4\,N_I \times p_{IE}$ inhibitory recurrent synaptic inputs. Furthermore, each inhibitory neuron receives $N_E \times p_{EI}$ excitatory inputs. Due to the small network size, inhibitory to inhibitory neuron connections are omitted ($p_{II} = 0$). The values for all other synaptic weights are sampled from a log normal distribution, in line with experiments (Song et al. 2005, Loewenstein et al. 2011), with $\mu = 1.0$ and $\sigma = 0.1$.

The initial values of the inhibitory synaptic weights are set to ten times weaker than the excitatory weights. Furthermore, the inhibitory synaptic weight update Δw_{ji} has a multiplicative weight dependence, such that:

$$
\begin{aligned}
w_{ji} &\leftarrow (W_{max} - w_{ji}) \times \Delta w_{ji} & \text{when } \Delta w_{ji} > 0 \\
w_{ji} &\leftarrow w_{ji} \times \Delta w_{ji} & \text{when } \Delta w_{ji} < 0
\end{aligned}
\tag{9}
$$

where W_{max} is the is the maximum inhibitory synaptic weight. The inhibitory learning is turned off during the first 15 seconds of the simulation.

Random neuron input generation

Each neuron in the network is randomly connected with a probability of $p_{ex} = 0.2$ to a subset of the N_{ex} external inputs, which are modelled as Poisson process with a mean firing rate F. To generate sufficient network activity, the synaptic weights from the external inputs to the excitatory and inhibitory neurons are 2.5 times stronger than the mean recurrent excitatory weight. For the simulation in Fig 2.A, the values of the synaptic weights from the external inputs to two excitatory neurons are increased by 50%.

Memory protocol

The same network as above is used in the simulation. After the network activity stabilises (600 s), the recurrent synapses between a selected subset of N^E (12/80) are increased by a factor of 5. After the network reaches steady state again (1200 s), the values of the synaptic weights from the N_{ex}^E to two neurons in the assembly are increased by 50%.

Inhibitory spike-timing dependent plasticity (iSTDP)

With iSTDP (Vogels et al. 2011), the synaptic weight w_{ji} from presynaptic inhibitory neuron i and the postsynaptic excitatory neuron j follows:

$$
\begin{aligned}
w_{ji} &\leftarrow w_{ji} + \eta_{iSTDP}(x_j - \alpha) \qquad \text{when } \textbf{pre}\text{synaptic neuron } i \text{ spikes} \\
w_{ji} &\leftarrow w_{ji} + \eta_{iSTDP}x_i \qquad \text{when } \textbf{post}\text{synaptic neuron } j \text{ spikes}
\end{aligned}
\tag{10}
$$

where η_{iSTDP} is the learning rate, α is the depression factor and $x_{i/j}$ is the neuron synaptic trace, defined as:

$$
\tau_{STDP}\frac{dx_{i/j}}{dt} = -x_{i/j} + \delta(t - t_{spike})
\tag{11}
$$

where τ_{iSTDP} is the learning window time constant and t_{spike} is the spike time.

Code

In all the simulations, we use Euler integration with step size Δt of 1 ms. The Python code will be made freely available after publication (GitHub and ModelDB) and is given to the reviewer.

Acknowledgements

Parameters summary

Parameters common across both simulated networks.

Neuron Model		
V_{REST}	- 60 mV	Resting membrane potential
Θ_m	- 50 mV	Membrane potential spiking threshold
R	100 $M\Omega$	Membrane resistance
t_{ref}	2 ms	Absolute refractory period
τ_m	20 ms	Membrane time constant
I_{ex}	0 A	Default external current

Synapse Model		
$\bar{g}$	1 nS	Basic weight unit
V^E	0 mV	Excitatory reversal potential
V^I	- 80 mV	Inhibitory reversal potential
τ_E	5 ms	Decay constant of AMPA-type conductance
τ_I	10 ms	Decay constant of GABA-type conductance

IDIP		
τ_{IDIP}	160 ms	IDIP decay constant

Simulation		
Δt	1 ms	Integration time step size

Hippocampal Network Model			
CA3 neurons	N_{CA3}	10	Size of the CA3 excitatory population
CA1 neurons	N_E	100	Size of the CA1 excitatory population
	N_I	20	Size of the CA1 inhibitory population
	N_g	10	Number of excitatory neuron groups
Position modulated input	N_{pc}	10	Number of place fields
	σ_{pc}	6.54 a.u.	Tuning width
	A_c	200 pA	Current amplitude
External current	I_{ex}^E	0.01 pA	Current to the excitatory neurons
	I_{ex}^I	0.5 pA	Current to the inhibitory neurons
Synaptic weights	W_{EI}	2.0	E to I synaptic weight
	W_{IE}	0.1	Initial I to E synaptic weight
IDIP	η_{IDIP}	10	IDIP learning rate
	θ_{in}	200 nS	Inhibitory neuron target input
Excitatory plasticity	τ_{hebb}	20 ms	Learning window time constant
	W_{max}	1.5	Maximum E to E synaptic weight
	η_{hebb}	0.01 s^{-1}	Excitatory Hebbian term learning rate
	η_{homeo}	0.001 s^{-1}	Excitatory homeostatic term learning rate
	θ_{homeo}	5.2	Homeostatic target sum of weights

Recurrent Network Model			
Neurons	N_{ex}	100	Size of the input population
	N_E	80	Size of the excitatory population
	N_I	20	Size of the inhibitory population
Probability of connections	p_{ex}	0.2	External input to the recurrent
	p_{EE}	0.1	Excitatory to excitatory connectivity
	p_{EI}	0.25	Excitatory to inhibitory connectivity
	p_{IE}	0.25	Inhibitory to excitatory connectivity
	p_{II}	0	Inhibitory to inhibitory connectivity
External input	F	10 Hz	Mean firing rate of external Poisson input
Synaptic weights	μ	1.0	Mean of the sampled distribution
	σ	0.05	s.d. of the sampled distribution
IDIP	η_{IDIP}	1e5 s^{-1}	IDIP learning rate
	θ_{in}	550 nS	Inhibitory neuron target input
	W_{max}	1.0	Maximum I to E synaptic weight
iSTDP	τ_{iSTDP}	20 ms	Learning window time constant
	η_{iSDTP}	0.05 s^{-1}	iSTDP learning rate
	α	0.2	Depression factor

References

Ali, A. B., Deuchars, J., Pawelzik, H. & Thomson, A. M. (1998), 'Ca1 pyramidal to basket and bistratified cell epsps: dual intracellular recordings in rat hippocampal slices', *The Journal of Physiology* **507**(1), 201–217.

Barnes, S. J., Sammons, R. P., Jacobsen, R. I., Mackie, J., Keller, G. B. & Keck, T. (2015), 'Subnetwork-specific homeostatic plasticity in mouse visual cortex in vivo', *Neuron* **86**(5), 1290–1303.

Barron, H. C., Vogels, T. P., Behrens, T. E. & Ramaswami, M. (2017), 'Inhibitory engrams in perception and memory', *Proceedings of the National Academy of Sciences* **114**(26), 6666–6674.

Bezaire, M. J. & Soltesz, I. (2013), 'Quantitative assessment of ca1 local circuits: knowledge base for interneuron-pyramidal cell connectivity', *Hippocampus* **23**(9), 751–785.

Bienenstock, E. L., Cooper, L. N. & Munro, P. W. (1982), 'Theory for the development of neuron selectivity: orientation specificity and binocular interaction in visual cortex', *Journal of Neuroscience* **2**(1), 32–48.

Bock, D. D., Lee, W.-C. A., Kerlin, A. M., Andermann, M. L., Hood, G., Wetzel, A. W., Yurgenson, S., Soucy, E. R., Kim, H. S. & Reid, R. C. (2011), 'Network anatomy and in vivo physiology of visual cortical neurons', *Nature* **471**(7337), 177–182.

Buzsáki, G. (2010), 'Neural syntax: cell assemblies, synapsembles, and readers', *Neuron* **68**(3), 362–385.

Chen, J. L., Lin, W. C., Cha, J. W., So, P. T., Kubota, Y. & Nedivi, E. (2011), 'Structural basis for the role of inhibition in facilitating adult brain plasticity', *Nature neuroscience* **14**(5), 587.

Clopath, C., Vogels, T. P., Froemke, R. C. & Sprekeler, H. (2016), 'Receptive field formation by interacting excitatory and inhibitory synaptic plasticity', *BioRxiv* p. 066589.

Cornford, J. H., Mercier, M. S., Leite, M., Magloire, V., Häusser, M. & Kullmann, D. M. (2019), 'Dendritic nmda receptors in parvalbumin neurons enable strong and stable neuronal assemblies', *Elife* **8**.

Csicsvari, J., Czurko, A., Hirase, H. & Buzsaki, G. (1998), Monosynaptic interactions between ca1 pyramidal cells and interneuron in the behaving rat., *in* 'European Journal of Neuroscience',

Vol. 10, BLACKWELL SCIENCE LTD PO BOX 88, OSNEY MEAD, OXFORD OX2 0NE, OXON, ENGLAND, pp. 63–63.

Csicsvari, J., Hirase, H., Czurko, A. & Buzsáki, G. (1998), 'Reliability and state dependence of pyramidal cell–interneuron synapses in the hippocampus: an ensemble approach in the behaving rat', *Neuron* **21**(1), 179–189.

Das, S., Sadanandappa, M. K., Dervan, A., Larkin, A., Lee, J. A., Sudhakaran, I. P., Priya, R., Heidari, R., Holohan, E. E., Pimentel, A. et al. (2011), 'Plasticity of local gabaergic interneurons drives olfactory habituation', *Proceedings of the National Academy of Sciences* **108**(36), E646–E654.

De Gois, S., Schäfer, M. K.-H., Defamie, N., Chen, C., Ricci, A., Weihe, E., Varoqui, H. & Erickson, J. D. (2005), 'Homeostatic scaling of vesicular glutamate and gaba transporter expression in rat neocortical circuits', *Journal of Neuroscience* **25**(31), 7121–7133.

Desai, N. S., Cudmore, R. H., Nelson, S. B. & Turrigiano, G. G. (2002), 'Critical periods for experience-dependent synaptic scaling in visual cortex', *Nature neuroscience* **5**(8), 783–789.

Desai, N. S., Rutherford, L. C. & Turrigiano, G. G. (1999), 'Plasticity in the intrinsic excitability of cortical pyramidal neurons', *Nature neuroscience* **2**(6), 515–520.

Deuchars, J. & Thomson, A. (1996), 'Ca1 pyramid-pyramid connections in rat hippocampus in vitro: dual intracellular recordings with biocytin filling', *Neuroscience* **74**(4), 1009–1018.

Dickman, D. & Wondolowski, J. (2013), 'Emerging links between homeostatic synaptic plasticity and neurological disease', *Frontiers in cellular neuroscience* **7**, 223.

Dupret, D., O'Neill, J. & Csicsvari, J. (2013), 'Dynamic reconfiguration of hippocampal interneuron circuits during spatial learning', *Neuron* **78**(1), 166–180.

D'amour, J. A. & Froemke, R. C. (2015), 'Inhibitory and excitatory spike-timing-dependent plasticity in the auditory cortex', *Neuron* **86**(2), 514–528.

English, D. F., McKenzie, S., Evans, T., Kim, K., Yoon, E. & Buzsáki, G. (2017), 'Pyramidal cell-interneuron circuit architecture and dynamics in hippocampal networks', *Neuron* **96**(2), 505–520.

Epsztein, J., Brecht, M. & Lee, A. K. (2011), 'Intracellular determinants of hippocampal ca1 place and silent cell activity in a novel environment', *Neuron* **70**(1), 109–120.

Fino, E. & Yuste, R. (2011), 'Dense inhibitory connectivity in neocortex', *Neuron* **69**(6), 1188–1203.

Frank, C. A., Kennedy, M. J., Goold, C. P., Marek, K. W. & Davis, G. W. (2006), 'Mechanisms underlying the rapid induction and sustained expression of synaptic homeostasis', *Neuron* **52**(4), 663–677.

Freund, T. F. & Buzsaki, G. (1996), 'Interneurons of the hippocampus', *Hippocampus* **6**(4), 347–470.

Gainey, M. A., Aman, J. W. & Feldman, D. E. (2018), 'Rapid disinhibition by adjustment of pv intrinsic excitability during whisker map plasticity in mouse s1', *Journal of Neuroscience* **38**(20), 4749–4761.

Gainey, M. A. & Feldman, D. E. (2017), 'Multiple shared mechanisms for homeostatic plasticity in rodent somatosensory and visual cortex', *Philosophical Transactions of the Royal Society B: Biological Sciences* **372**(1715), 20160157.

Gallinaro, J. V. & Rotter, S. (2018), 'Associative properties of structural plasticity based on firing rate homeostasis in recurrent neuronal networks', *Scientific reports* **8**(1), 1–13.

Gasparini, S. & Magee, J. C. (2006), 'State-dependent dendritic computation in hippocampal ca1 pyramidal neurons', *Journal of Neuroscience* **26**(7), 2088–2100.

Geisler, C., Robbe, D., Zugaro, M., Sirota, A. & Buzsáki, G. (2007), 'Hippocampal place cell assemblies are speed-controlled oscillators', *Proceedings of the National Academy of Sciences* **104**(19), 8149–8154.

Ghandour, K., Ohkawa, N., Fung, C. C. A., Asai, H., Saitoh, Y., Takekawa, T., Okubo-Suzuki, R., Soya, S., Nishizono, H., Matsuo, M. et al. (2019), 'Orchestrated ensemble activities constitute a hippocampal memory engram', *Nature communications* **10**(1), 1–14.

Glazewski, S., Greenhill, S. & Fox, K. (2017), 'Time-course and mechanisms of homeostatic plasticity in layers 2/3 and 5 of the barrel cortex', *Philosophical Transactions of the Royal Society B: Biological Sciences* **372**(1715), 20160150.

Goel, A. & Lee, H.-K. (2007), 'Persistence of experience-induced homeostatic synaptic plasticity through adulthood in superficial layers of mouse visual cortex', *Journal of Neuroscience* **27**(25), 6692–6700.

Grienberger, C., Milstein, A. D., Bittner, K. C., Romani, S. & Magee, J. C. (2017), 'Inhibitory suppression of heterogeneously tuned excitation enhances spatial coding in ca1 place cells', *Nature neuroscience* **20**(3), 417–426.

Gulyás, A. I., Megıas, M., Emri, Z. & Freund, T. F. (1999), 'Total number and ratio of excitatory and inhibitory synapses converging onto single interneurons of different types in the ca1 area of the rat hippocampus', *Journal of Neuroscience* **19**(22), 10082–10097.

Gupta, A., Wang, Y. & Markram, H. (2000), 'Organizing principles for a diversity of gabaergic interneurons and synapses in the neocortex', *Science* **287**(5451), 273–278.

Haas, J. S., Nowotny, T. & Abarbanel, H. D. (2006), 'Spike-timing-dependent plasticity of inhibitory synapses in the entorhinal cortex', *Journal of neurophysiology* **96**(6), 3305–3313.

Han, J.-H., Kushner, S. A., Yiu, A. P., Cole, C. J., Matynia, A., Brown, R. A., Neve, R. L., Guzowski, J. F., Silva, A. J. & Josselyn, S. A. (2007), 'Neuronal competition and selection during memory formation', *science* **316**(5823), 457–460.

Harris, K. D. & Shepherd, G. M. (2015), 'The neocortical circuit: themes and variations', *Nature neuroscience* **18**(2), 170–181.

Hartline, H. K. & Ratliff, F. (1957), 'Inhibitory interaction of receptor units in the eye of limulus', *The Journal of general physiology* **40**(3), 357–376.

Hartman, K. N., Pal, S. K., Burrone, J. & Murthy, V. N. (2006), 'Activity-dependent regulation of inhibitory synaptic transmission in hippocampal neurons', *Nature neuroscience* **9**(5), 642–649.

Hengen, K. B., Lambo, M. E., Van Hooser, S. D., Katz, D. B. & Turrigiano, G. G. (2013), 'Firing rate homeostasis in visual cortex of freely behaving rodents', *Neuron* **80**(2), 335–342.

Hennequin, G., Agnes, E. J. & Vogels, T. P. (2017), 'Inhibitory plasticity: balance, control, and codependence', *Annual Review of Neuroscience* **40**, 557–579.

Hirase, H., Leinekugel, X., Czurkó, A., Csicsvari, J. & Buzsáki, G. (2001), 'Firing rates of hippocampal neurons are preserved during subsequent sleep episodes and modified by novel awake experience', *Proceedings of the National Academy of Sciences* **98**(16), 9386–9390.

Hofer, S. B., Ko, H., Pichler, B., Vogelstein, J., Ros, H., Zeng, H., Lein, E., Lesica, N. A. & Mrsic-Flogel, T. D. (2011), 'Differential connectivity and response dynamics of excitatory and inhibitory neurons in visual cortex', *Nature neuroscience* **14**(8), 1045.

32

Homayoun, H. & Moghaddam, B. (2007), 'Nmda receptor hypofunction produces opposite effects on prefrontal cortex interneurons and pyramidal neurons', *Journal of Neuroscience* **27**(43), 11496–11500.

Hughes, D. I., Bannister, A. P., Pawelzik, H. & Thomson, A. M. (2000), 'Double immunofluorescence, peroxidase labelling and ultrastructural analysis of interneurones following prolonged electrophysiological recordings in vitro', *Journal of neuroscience methods* **101**(2), 107–116.

Jackson, M. E., Homayoun, H. & Moghaddam, B. (2004), 'Nmda receptor hypofunction produces concomitant firing rate potentiation and burst activity reduction in the prefrontal cortex', *Proceedings of the National Academy of Sciences* **101**(22), 8467–8472.

Joseph, A. & Turrigiano, G. G. (2017), 'All for one but not one for all: excitatory synaptic scaling and intrinsic excitability are coregulated by camkiv, whereas inhibitory synaptic scaling is under independent control', *Journal of Neuroscience* **37**(28), 6778–6785.

Keck, T., Scheuss, V., Jacobsen, R. I., Wierenga, C. J., Eysel, U. T., Bonhoeffer, T. & Hübener, M. (2011), 'Loss of sensory input causes rapid structural changes of inhibitory neurons in adult mouse visual cortex', *Neuron* **71**(5), 869–882.

Kerlin, A. M., Andermann, M. L., Berezovskii, V. K. & Reid, R. C. (2010), 'Broadly tuned response properties of diverse inhibitory neuron subtypes in mouse visual cortex', *Neuron* **67**(5), 858–871.

Kirkwood, A., Rioult, M. G. & Bear, M. F. (1996), 'Experience-dependent modification of synaptic plasticity in visual cortex', *Nature* **381**(6582), 526–528.

Korotkova, T., Fuchs, E. C., Ponomarenko, A., von Engelhardt, J. & Monyer, H. (2010), 'Nmda receptor ablation on parvalbumin-positive interneurons impairs hippocampal synchrony, spatial representations, and working memory', *Neuron* **68**(3), 557–569.

Kuhlman, S. J., Olivas, N. D., Tring, E., Ikrar, T., Xu, X. & Trachtenberg, J. T. (2013), 'A disinhibitory microcircuit initiates critical-period plasticity in the visual cortex', *Nature* **501**(7468), 543–546.

Lambo, M. E. & Turrigiano, G. G. (2013), 'Synaptic and intrinsic homeostatic mechanisms cooperate to increase l2/3 pyramidal neuron excitability during a late phase of critical period plasticity', *Journal of Neuroscience* **33**(20), 8810–8819.

Lau, C. G. & Murthy, V. N. (2012), 'Activity-dependent regulation of inhibition via gad67', *Journal of Neuroscience* **32**(25), 8521–8531.

Laughlin, S. (1981), 'A simple coding procedure enhances a neuron's information capacity', *Zeitschrift für Naturforschung c* **36**(9-10), 910–912.

Le Roux, N., Cabezas, C., Böhm, U. L. & Poncer, J. C. (2013), 'Input-specific learning rules at excitatory synapses onto hippocampal parvalbumin-expressing interneurons', *The Journal of physiology* **591**(7), 1809–1822.

Li, L., Gainey, M. A., Goldbeck, J. E. & Feldman, D. E. (2014), 'Rapid homeostasis by disinhibition during whisker map plasticity', *Proceedings of the National Academy of Sciences* **111**(4), 1616–1621.

Loewenstein, Y., Kuras, A. & Rumpel, S. (2011), 'Multiplicative dynamics underlie the emergence of the log-normal distribution of spine sizes in the neocortex in vivo', *Journal of Neuroscience* **31**(26), 9481–9488.

Losonczy, A. & Magee, J. C. (2006), 'Integrative properties of radial oblique dendrites in hippocampal ca1 pyramidal neurons', *Neuron* **50**(2), 291–307.

Ma, W.-p., Liu, B.-h., Li, Y.-t., Huang, Z. J., Zhang, L. I. & Tao, H. W. (2010), 'Visual representations by cortical somatostatin inhibitory neurons—selective but with weak and delayed responses', *Journal of Neuroscience* **30**(43), 14371–14379.

Maffei, A., Nataraj, K., Nelson, S. B. & Turrigiano, G. G. (2006), 'Potentiation of cortical inhibition by visual deprivation', *Nature* **443**(7107), 81–84.

Maffei, A., Nelson, S. B. & Turrigiano, G. G. (2004), 'Selective reconfiguration of layer 4 visual cortical circuitry by visual deprivation', *Nature neuroscience* **7**(12), 1353–1359.

Maffei, A. & Turrigiano, G. (2008), 'The age of plasticity: developmental regulation of synaptic plasticity in neocortical microcircuits', *Progress in brain research* **169**, 211–223.

Markram, H., Toledo-Rodriguez, M., Wang, Y., Gupta, A., Silberberg, G. & Wu, C. (2004), 'Interneurons of the neocortical inhibitory system', *Nature reviews neuroscience* **5**(10), 793.

Meyer, H. S., Schwarz, D., Wimmer, V. C., Schmitt, A. C., Kerr, J. N., Sakmann, B. & Helmstaedter, M. (2011), 'Inhibitory interneurons in a cortical column form hot zones of inhibition in layers 2 and 5a', *Proceedings of the National Academy of Sciences* **108**(40), 16807–16812.

Mizuseki, K. & Buzsáki, G. (2013), 'Preconfigured, skewed distribution of firing rates in the hippocampus and entorhinal cortex', *Cell reports* **4**(5), 1010–1021.

Naumann, L. B. & Sprekeler, H. (2020), 'Presynaptic inhibition rapidly stabilises recurrent excitation in the face of plasticity', *bioRxiv* .

Niell, C. M. & Stryker, M. P. (2008), 'Highly selective receptive fields in mouse visual cortex', *Journal of Neuroscience* **28**(30), 7520–7536.

O'Keefe, J. (1976), 'Place units in the hippocampus of the freely moving rat', *Experimental neurology* **51**(1), 78–109.

O'Keefe, J. & Dostrovsky, J. (1971), 'The hippocampus as a spatial map: preliminary evidence from unit activity in the freely-moving rat.', *Brain research* .

O'keefe, J. & Nadel, L. (1978), *The hippocampus as a cognitive map*, Oxford: Clarendon Press.

Pacheco, A. T., Bottorff, J. & Turrigiano, G. G. (2019), 'Sleep promotes downward firing rate homeostasis', *bioRxiv* p. 827832.

Packer, A. M. & Yuste, R. (2011), 'Dense, unspecific connectivity of neocortical parvalbumin-positive interneurons: a canonical microcircuit for inhibition?', *Journal of Neuroscience* **31**(37), 13260–13271.

Pan-Vazquez, A., Wefelmeyer, W., Sabater, V. G., Neves, G. & Burrone, J. (2020), 'Activity-dependent plasticity of axo-axonic synapses at the axon initial segment', *Neuron* .

Paraskevopoulou, F., Herman, M. A. & Rosenmund, C. (2019), 'Glutamatergic innervation onto striatal neurons potentiates gabaergic synaptic output', *Journal of Neuroscience* **39**(23), 4448–4460.

Peng, Y.-R., Zeng, S.-Y., Song, H.-L., Li, M.-Y., Yamada, M. K. & Yu, X. (2010), 'Postsynaptic spiking homeostatically induces cell-autonomous regulation of inhibitory inputs via retrograde signaling', *Journal of Neuroscience* **30**(48), 16220–16231.

Perrinet, L. U. (2010), 'Role of homeostasis in learning sparse representations', *Neural computation* **22**(7), 1812–1836.

Pfeffer, C. K., Xue, M., He, M., Huang, Z. J. & Scanziani, M. (2013), 'Inhibition of inhibition in visual cortex: the logic of connections between molecularly distinct interneurons', *Nature neuroscience* **16**(8), 1068–1076.

Pignatelli, M., Ryan, T. J., Roy, D. S., Lovett, C., Smith, L. M., Muralidhar, S. & Tonegawa, S. (2019), 'Engram cell excitability state determines the efficacy of memory retrieval', *Neuron* **101**(2), 274–284.

Poirazi, P. & Mel, B. W. (2001), 'Impact of active dendrites and structural plasticity on the memory capacity of neural tissue', *Neuron* **29**(3), 779–796.

Poirazi, P. & Papoutsi, A. (2020), 'Illuminating dendritic function with computational models', *Nature Reviews Neuroscience* pp. 1–19.

Schoenenberger, P., O'Neill, J. & Csicsvari, J. (2016), 'Activity-dependent plasticity of hippocampal place maps', *Nature communications* **7**, 11824.

Slomowitz, E., Styr, B., Vertkin, I., Milshtein-Parush, H., Nelken, I., Slutsky, M. & Slutsky, I. (2015), 'Interplay between population firing stability and single neuron dynamics in hippocampal networks', *Elife* **4**, e04378.

Sohya, K., Kameyama, K., Yanagawa, Y., Obata, K. & Tsumoto, T. (2007), 'Gabaergic neurons are less selective to stimulus orientation than excitatory neurons in layer ii/iii of visual cortex, as revealed by in vivo functional ca2+ imaging in transgenic mice', *Journal of Neuroscience* **27**(8), 2145–2149.

Song, S., Sjöström, P. J., Reigl, M., Nelson, S. & Chklovskii, D. B. (2005), 'Highly nonrandom features of synaptic connectivity in local cortical circuits', *PLoS biology* **3**(3).

Steinert, J. R., Kopp-Scheinpflug, C., Baker, C., Challiss, R. J., Mistry, R., Haustein, M. D., Griffin, S. J., Tong, H., Graham, B. P. & Forsythe, I. D. (2008), 'Nitric oxide is a volume transmitter regulating postsynaptic excitability at a glutamatergic synapse', *Neuron* **60**(4), 642–656.

Steinert, J. R., Robinson, S. W., Tong, H., Haustein, M. D., Kopp-Scheinpflug, C. & Forsythe, I. D. (2011), 'Nitric oxide is an activity-dependent regulator of target neuron intrinsic excitability', *Neuron* **71**(2), 291–305.

Stemmler, M. & Koch, C. (1999), 'How voltage-dependent conductances can adapt to maximize the information encoded by neuronal firing rate', *Nature neuroscience* **2**(6), 521–527.

Stuart, G. J. & Spruston, N. (2015), 'Dendritic integration: 60 years of progress', *Nature neuroscience* **18**(12), 1713–1721.

Sweeney, Y., Kotaleski, J. H. & Hennig, M. H. (2015), 'A diffusive homeostatic signal maintains neural heterogeneity and responsiveness in cortical networks', *PLoS computational biology* **11**(7).

Tamamaki, N. & Tomioka, R. (2010), 'Long-range gabaergic connections distributed throughout the neocortex and their possible function', *Frontiers in neuroscience* **4**, 202.

Thomson, A. M. & Radpour, S. (1991), 'Excitatory connections between ca1 pyramidal cells revealed by spike triggered averaging in slices of rat hippocampus are partially nmda receptor mediated', *European journal of neuroscience* **3**(6), 587–601.

Tonegawa, S. (2019), 'Engram cell excitability state determines the efficacy of memory retrieval', *Neuron* **101**, 1–11.

Trouche, S., Perestenko, P. V., van de Ven, G. M., Bratley, C. T., McNamara, C. G., Campo-Urriza, N., Black, S. L., Reijmers, L. G. & Dupret, D. (2016), 'Recoding a cocaine-place memory engram to a neutral engram in the hippocampus', *Nature neuroscience* **19**(4), 564–567.

Turrigiano, G. G., Leslie, K. R., Desai, N. S., Rutherford, L. C. & Nelson, S. B. (1998), 'Activity-dependent scaling of quantal amplitude in neocortical neurons', *Nature* **391**(6670), 892–896.

Turrigiano, G. G. & Nelson, S. B. (2004), 'Homeostatic plasticity in the developing nervous system', *Nature reviews neuroscience* **5**(2), 97–107.

Udakis, M., Pedrosa, V., Chamberlain, S. E., Clopath, C. & Mellor, J. R. (2019), 'Interneuron-specific plasticity at parvalbumin and somatostatin inhibitory synapses onto ca1 pyramidal neurons shapes hippocampal output', *bioRxiv* p. 774562.

van Versendaal, D., Rajendran, R., Saiepour, M. H., Klooster, J., Smit-Rigter, L., Sommeijer, J.-P., De Zeeuw, C. I., Hofer, S. B., Heimel, J. A. & Levelt, C. N. (2012), 'Elimination of inhibitory synapses is a major component of adult ocular dominance plasticity', *Neuron* **74**(2), 374–383.

Vogels, T. P., Sprekeler, H., Zenke, F., Clopath, C. & Gerstner, W. (2011), 'Inhibitory plasticity balances excitation and inhibition in sensory pathways and memory networks', *Science* **334**(6062), 1569–1573.

Wang, Y., Gupta, A., Toledo-Rodriguez, M., Wu, C. Z. & Markram, H. (2002), 'Anatomical, physiological, molecular and circuit properties of nest basket cells in the developing somatosensory cortex', *Cerebral cortex* **12**(4), 395–410.

Wilson, D. E., Smith, G. B., Jacob, A. L., Walker, T., Dimidschstein, J., Fishell, G. & Fitzpatrick, D. (2017), 'Gabaergic neurons in ferret visual cortex participate in functionally specific networks', *Neuron* **93**(5), 1058–1065.

Wilson, M. A. & McNaughton, B. L. (1993), 'Dynamics of the hippocampal ensemble code for space', *Science* **261**(5124), 1055–1058.

Wohrer, A., Humphries, M. D. & Machens, C. K. (2013), 'Population-wide distributions of neural activity during perceptual decision-making', *Progress in neurobiology* **103**, 156–193.

Woodin, M. A., Ganguly, K. & Poo, M.-m. (2003), 'Coincident pre-and postsynaptic activity modifies gabaergic synapses by postsynaptic changes in cl- transporter activity', *Neuron* **39**(5), 807–820.

Wu, Y., Hengen, K. B., Turrigiano, G. G. & Gjorgjieva, J. (2019), 'Homeostatic mechanisms regulate distinct aspects of cortical circuit dynamics', *bioRxiv* p. 790410.

Yassin, L., Benedetti, B. L., Jouhanneau, J.-S., Wen, J. A., Poulet, J. F. & Barth, A. L. (2010), 'An embedded subnetwork of highly active neurons in the neocortex', *Neuron* **68**(6), 1043–1050.

Yin, J. & Yuan, Q. (2015), 'Structural homeostasis in the nervous system: a balancing act for wiring plasticity and stability', *Frontiers in cellular neuroscience* **8**, 439.

Zariwala, H. A., Madisen, L., Ahrens, K. F., Bernard, A., Lein, E. S., Jones, A. R. & Zeng, H. (2011), 'Visual tuning properties of genetically identified layer 2/3 neuronal types in the primary visual cortex of cre-transgenic mice', *Frontiers in systems neuroscience* **4**, 162.

Zenke, F., Hennequin, G. & Gerstner, W. (2013), 'Synaptic plasticity in neural networks needs homeostasis with a fast rate detector', *PLoS computational biology* **9**(11).

Zhang, Y., Behrens, M. M. & Lisman, J. E. (2008), 'Prolonged exposure to nmdar antagonist suppresses inhibitory synaptic transmission in prefrontal cortex', *Journal of neurophysiology* **100**(2), 959–965.

Znamenskiy, P., Kim, M.-H., Muir, D. R., Iacaruso, M. F., Hofer, S. B. & Mrsic-Flogel, T. D. (2018), 'Functional selectivity and specific connectivity of inhibitory neurons in primary visual cortex', *bioRxiv* p. 294835.